MASTER

LBL-11239

CONF-800850--4

Lawrence Berkeley Laboratory

UNIVERSITY OF CALIFORNIA

Materials & Molecular Research Division

Presented at the International Conference on Hydrogen Effects on Metal, Jackson Hole, WY, August 26-30, 1980

DEVELOPMENT OF A HIGH STRENGTH, HYDROGEN-RESISTANT AUSTENITIC ALLOY

K.M. Chang, D.H. Klahn, and J.W. Morris, Jr.

August 1980

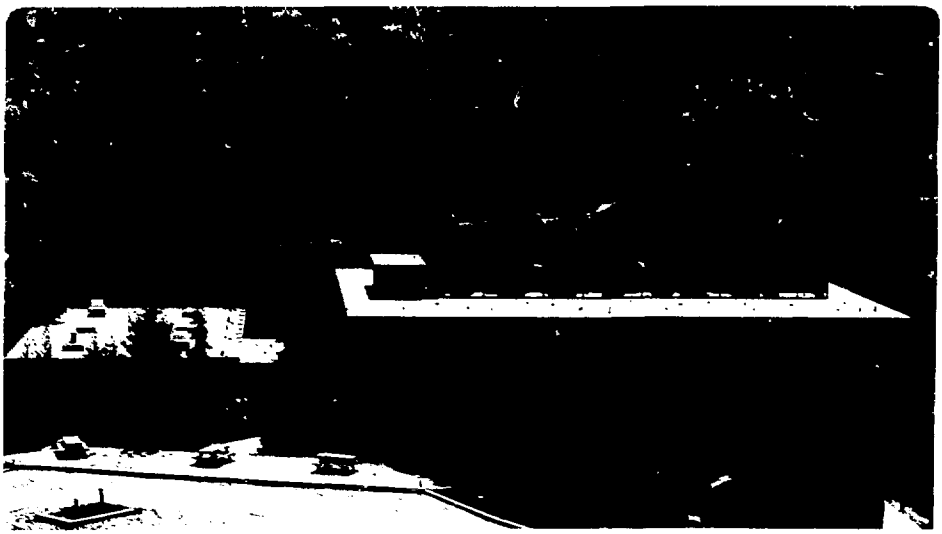

DISTRIBUTION OF THIS DOCUMENT IS UNLIMITED

Prepared for the U.S. Department of Energy under Contract W-7405-ENG-48

DISCLAIMER

DEVELOPMENT OF A HIGH STRENGTH, HYDROGEN-RESISTANT AUSTENITIC ALLOY

K. M. Chang, D. H. Klahn and J. W. Morris, Jr.
Lawrence Berkeley Laboratory and
Dept. of Materials Science and Mineral Eng.,
University of California,
Berkeley, California 94720

Abstract

Research toward high-strength, high toughness non-magnetic steels for use in the retaining rings of large electrical generators led to the development of a Ta-modified iron-based superalloy which combines high strength with good toughness after suitable aging. The alloy did, however, show some degradation in fatigue resistance in gaseous hydrogen. This sensitivity was associated with a deformation-induced martensitic transformation near the fracture surface. The addition of a small amount of chromium to the alloy suppressed the martensite transformation and led to a marked improvement in hydrogen resistance.

Introduction

The work reported here was done in the course of research toward a new high-strength non-magnetic steel for use in the retaining rings of large electrical generators. The constraints on the alloy required that it be hardenable through thermal processing to ~200 ksi (1380 MPa) yield strength with a residual fracture toughness, K_{Ic}, greater than 100 ksi $\sqrt{in.}$ (110 MPa $\sqrt{m}$) and that it not embrittle significantly in gaseous hydrogen, which is used to cool the generator.

Initial work focused on the attainment of the strength, toughness, and magnetic property objectives. The product of this work (1,2) was a tantalum-modified Fe-based superalloy, designated EPRI-E, of nominal composition Fe-36Ni-3Ti-3Ta-0.5Al-1.3Mo-0.3V-0.01B. If this alloy is upset cross-forged at 1100°C and then given a double-aging treatment of four hours at 750°C followed by four hours at 670°C, it is paramagnetic and has a yield strength of 1415 MPa (205 ksi) with 19% elongation and 67% reduction in area. Its plane strain fracture toughness (K_{Ic}) at this yield strength is ~120 MPa $\sqrt{m}$ (110 ksi $\sqrt{in}$). On the basis of these properties the alloy was subjected to hydrogen susceptibility tests, whose results, interpretation and consequences are the subject of this paper.

DISTRIBUTION OF THIS DOCUMENT IS UNL

Experimental

Laboratory 10kg ingots were induction-melted under partial helium pressure using high purity (99.9+) raw materials. After homogenization the ingots were upset cross-forged from 1150°C into plates, then water quenched. After machining to the appropriate size, the samples were sealed in stainless steel bags filled with argon for thermal treatments and were usually water-quenched afterwards.

The sensitivity of alloy mechanical properties to gaseous hydrogen was determined through tests conducted in a stainless steel chamber which could be evacuated to 10^{-3} torr and then backfilled with hydrogen to 0.8 atm. Evacuation insured that the hydrogen gas in the test chamber had a low concentration of active impurity gases such as O_2, H_2O, and N_2 (<100 ppm). Two types of specimen were tested at room temperature: notched tensile specimens and subsized compact tension specimens tested in a low cycle fatigue mode.

Results

Hydrogen Susceptibility

A series of notched tensile specimens were made from Alloy E to examine the hydrogen susceptibility. The results of testing are listed in Table I. Specimen EH-1 was tested in hydrogen at a crosshead speec of 3×10^{-3} in/min which gave a test time of 10 to 15 minutes. Specimens EH-2 and EH-4 were tested under the same conditions in air. The strength of these three specimens is virtually the same whether measured by the proportional limit or the ultimate load. However, a decrease in the total plastic extension suggested that the ductility of the hydrogen specimen EH-1 was less than that of the specimens tested in air. To investigate the effect of strain rate specimen EH-3 was tested in hydrogen at a lower crosshead speed. The total plastic extension was further reduced to only about one half that of the air specimens. The dependence of notch ductility on the strain rate not only suggests that alloy E is susceptible to hydrogen embrittlement but also indicates that hydrogen transport influences the embrittlement process (3).

Table 1. Notched Tensile Properties of Alloy E in Air and in Hydrogen.

Specimen	Environment	Cross-Head Speed (mm/sec)	Proportional Limit* MPa (ksi)	Ultimate Stress* MPa (ksi)	Plastic Extension ($\times 10^{-2}$mm)
EH-1	H_2 (0.8 atm)	1.27×10^{-3}	1898 (275)	2098 (304)	11.4
EH-2	Air	1.27×10^{-3}	1877 (272)	2105 (305)	17.5
EH-3	H_2 (0.8 atm)	1.27×10^{-4}	1932 (280)	2091 (303)	9.1
EH-4	Air	1.27×10^{-3}	1918 (278)	2091 (303)	17.3

* Stress based on actual area at root of notch.

Specimen data: Nominal gauge length - 12.7 mm
Nominal gauge diameter - 3.175 mm
Diameter at notch - 2.54 mm
Notch angle - 45°

Fatigue testing in which crack growth velocities in air and hydrogen are compared has been suggested by Nelson (4) as the most realistic and sensitive test for hydrogen sensitivity. The precracked compact tension specimen EHF-1 was first fatigued in air using an initial cycle $\Delta K=0.5k_{Ic}$, R=6, at a frequency of 1 cycle/sec. The maximum load was automatically adjusted to assure a constant crack opening. A record of load vs. fatigue cycle, taken at intervals of 500 cycles, is shown in Fig. 1. The slope of the curves is proportional to the crack growth velocity. After cycling specimen EHF-1 in air for 4500 cycles, the environment chamber was evacuated and then back-filled with 0.8 atm. hydrogen and the test continued for another 1000 cycles. Immediately following this environmental change, the load-cycle curve changed slope by a factor of 4.3. Specimen EHF-2 was then tested under the same conditions with cyclic loading hydrogen from the beginning. The crack growth velocity of EHF-2 was equal to that of EHF-1 in hydrogen. It was concluded that alloy E in the full-hardened condition is sensitive to hydrogen embrittlement.

Deformation-Induced Martensite

Magnetic measurements of various fracture surfaces of alloy E indicated an increase in the magnetic susceptibility. These and associated x-ray measurements (Table II) showed that the full-hardened alloy E was not completely stable with respect to mechanical deformation and some ferromagnetic α' martensite was induced on the fracture surfaces. The specimens broken in fatigue had a higher martensite fraction on the fracture surface than those broken in fracture toughness tests, despite the low stress intensity employed in fatigue tests. The presence of hydrogen during fatigue resulted in a still higher percentage of martensite, indicating that hydrogen promoted the transformation of austenite to martensite under deformation.

Table II. X-ray Diffraction Analysis on Various Fracture Surfaces of Alloy E.

Phase	Fatigue in H_2	Fatigue in Air	Rapid Fracture
Martensite (%)	86	73	61
Austenite (%)	14	27	39

Figure 2 shows the α' martensite phase formed near the fracture surfaces of fracture toughness and fatigue specimens, respectively. The mechanically-induced martensite takes the form of thin plates which appear in decreasing volume fraction with increasing distance from the fracture surface. The martensite-forming zone is much narrower on the fatigued surfaces than on the surface of the fracture toughness specimen, which presumably reflects the lower level of stress intensity in the fatigue tests. On the other hand, the transformation at the fracture surface is much more extensive in the fatigue tests and nearly covers the fracture surface; backscatter Mössbauer spectroscopic measurements, with a penetration depth of a few tens of angstroms, show 98% transformation on the surface of the speciment fatigued in hydrogen.

These data suggest a causal connection between the induced martensitic transformation and hydrogen susceptibility. Mechanistically, it is well known (5) that martensite is generally more sensitive to hydrogen embrittlement than austenite, hence an extensive martensitic transformation ahead of the propagating crack would be expected to promote crack growth in hydrogen. The data also suggest that the presence of hydrogen promotes the strain-induced transformation.

Alloy Modification

Given the clear association between the induced martensite transformation and sensitivity to hydrogen, a plausible alloy design approach to improve hydrogen resistance was to modify the alloy chemistry so as to increase stability with respect to martensitic transformation. Given the base composition of the alloy, the most obvious means for increasing austenite stability would be an increase in the nickel content. This approach is, however, precluded by the low temperature ferromagnetism of the alloy at higher nickel contents. Of the possible new element additions, chromium was immediately attractive since it both stabilizes the austenite phase (at least at lower concentrations) and enhances resistance to oxidation and corrosion. The acceptability of Cr modification was, however, dependent on the possibility of introducing it in significant concentration without compromising the desirable mechanical properties of the alloy.

To explore the consequences of Cr addition, a modified alloy was cast with nominal composition Fe-34.5Ni-5Cr-3Ti-3Ta-0.5Al-1.0Mo-0.3V-0.01B, and designated EPRI-T. The alloy differs from EPRI-E only through the Cr addition and a slight concommitant decrease in nickel content to compensate for the decrease in Fe. Age hardening studies revealed that the alloy shows a hardening response resembling that of EPRI-E and has virtually identical strength-toughness properties, as documented in Table III and Fig. 3. In the double-aged and fully hardened condition, however, alloy T is stable with respect to martensite transformation during normal mechanical testing at room temperature. No martensite phase was detected after either tensile or fracture toughness testing. The suppression of the martensitic transformation is also presumably responsible for the slight decrease in the total elongation of Alloy T relative to that of Alloy E.

Table III. Mechanical Properties of Double Aged Alloy E and Alloy T.

Alloy	Yield Strength MPa (ksi)	Tensile Strength MPa (ksi)	Elongation %	Reduction in Area T	Fracture Toughness MPa$\sqrt{m}$ (ksi$\sqrt{in}$)
E	1332 (193)	1587 (230)	24	60	114 (104)
T	1345 (195)	1539 (223)	18	53	115 (105)

Heat treatments: 750°C/3 hrs + 650°C/9 hrs

To evaluate the hydrogen sensitivity of EPRI-T, notched tensile and fatigue testing was conducted on the alloy after aging to ~200 ksi (1380 ksi) yield strength under conditions identical to those employed for testing of alloy E. Both the notched tensile properties and the fatigue crack growth rate in alloy T in 0.8 atm. hydrogen were essentially identical to those in air; no evident hydrogen sensitivity was found. Post-test examination of the fracture surfaces revealed no evidence for induced martensite.

Following these tests, fatigue pre-cracked compact tension specimens of alloy T were dead-weight loaded to stress intensities as high as 88 MPa $\sqrt{m}$ (80 ksi $\sqrt{in}$) and immersed in a 3.5% NaCl solution for periods up to one month. No evidence of crack growth was found.

Discussion

While the work reported here is not sufficient to establish a causal connection between the induced martensite transformation and the hydrogen sensitivity of alloy E, and while it is possible that the improvement in hydrogen resistance on addition of Cr reflects an influence on alloy chemistry as well as on phase stability, the parallel observations of an increase in the extent of martensitic transformation under fatigue conditions evidencing hydrogen embrittlement and the suppression of hydrogen susceptibility on stabilization with respect to strain-induced martensite strongly suggest a causal connection between the two phenomena and offer a promising approach for improving the hydrogen resistance of austenitic steels.

Acknowledgments

The authors are indebted to Dr. Howard G. Nelson, NASA-Ames Research Center, Moffitt Field, California, for assistance in providing the hydrogen test apparatus and helpful discussions. This work was supported by the Electric Power Research Institute under contract #RP-636-2, and made use of experimental facilities at the Lawrence Berkeley Laboratory supported by the Division of Material Science, Office of Basic Energy Sciences, U.S. Dept. of Energy under contract #W-7405-Eng-48.

References

1. J. W. Morris, Jr., K. M. Chang, D. H. Klahn, G. Thomas, and S. Jin: "Heat Treatment and Mechanical Properties of a Ta-Modified Fe-Base Superalloy," LBL Report No. 9799, Lawrence Berkeley Laboratory, Berkeley, CA., September, 1979.

2. J. W. Morris, Jr. and G. Thomas: EPRI Report FP-1061, Electric Power Research Institute, Palo Alto, CA., April, 1979.

3. J. K. Tien, A. W. Thompson, I. M. Bernstein, and R. J. Richards: Met. Trans. A., 7A (1976) p. 821.

4. H. G. Nelson, "Hydrogen Embrittlement Testing," ASTM STP 543, p. 152.

5. R. B. Benson, Jr., R. K. Dann, and L. W. Roberts, Jr.: Trans. TMS-AIME, 242 (1968) p. 2199.

FIGURE CAPTIONS

Fig. 1. Hydrogen effect on the fatigue crack growth rate of alloy E.

Fig. 2. Distribution of deformation-induced martensite on (a) fracture, (b) fatigue surface of alloy E.

Fig. 3. Yield strength-fracture toughness relations for alloys E and T after processing from the annealed (AN) and forged (A_f) conditions. The two alloys have essentially identical strength/toughness characteristics. Typical data for Inconel 718 and A-286 is also shown for comparison.

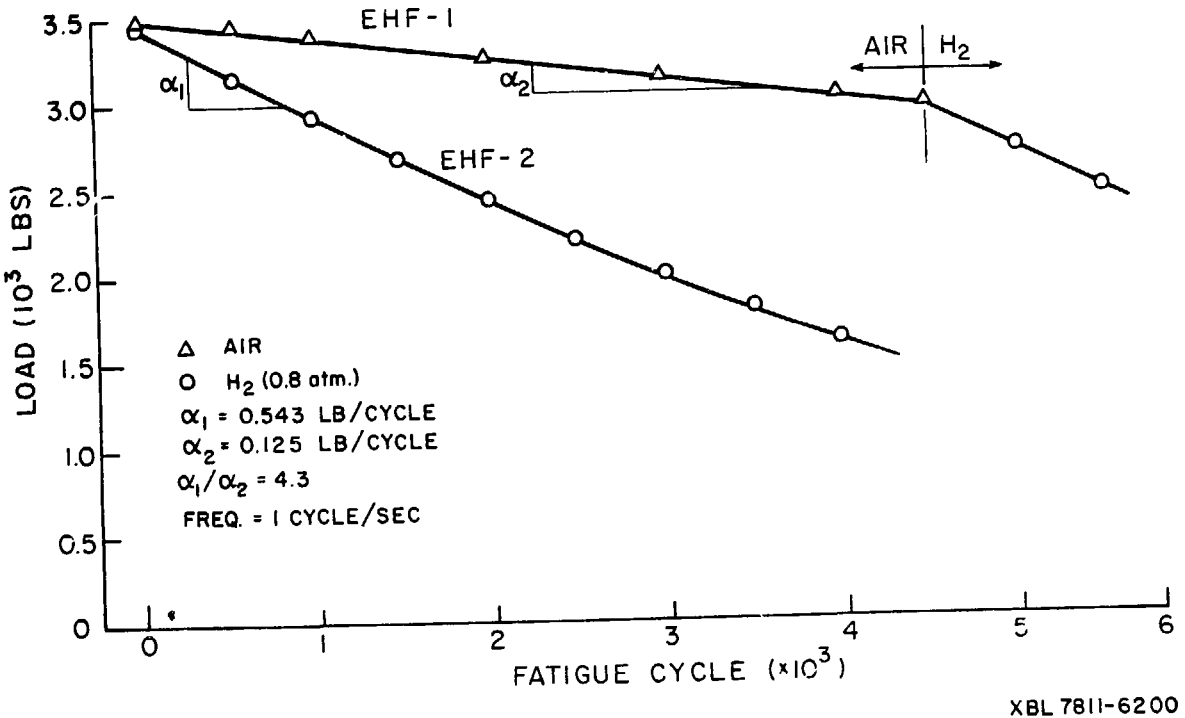
EHF-1
EHF-2
AIR
H_2
α_1
α_2
LOAD (10^3 LBS)
3.5
3.0
2.5
2.0
1.5
1.0
0.5
0
△ AIR
○ H_2 (0.8 atm.)
α_1 = 0.543 LB/CYCLE
α_2 = 0.125 LB/CYCLE
α_1/α_2 = 4.3
FREQ. = 1 CYCLE/SEC
0
1
2
3
4
5
6
FATIGUE CYCLE ($\times 10^3$)
XBL 7811-6200

Figure 1

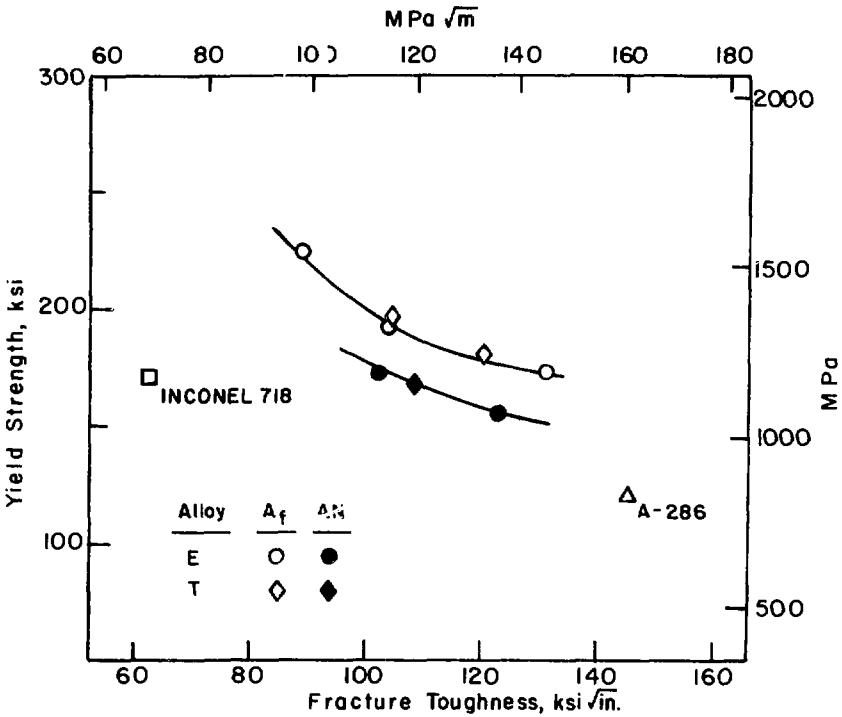

Figure 2

XBL 792-5852A

Fracture

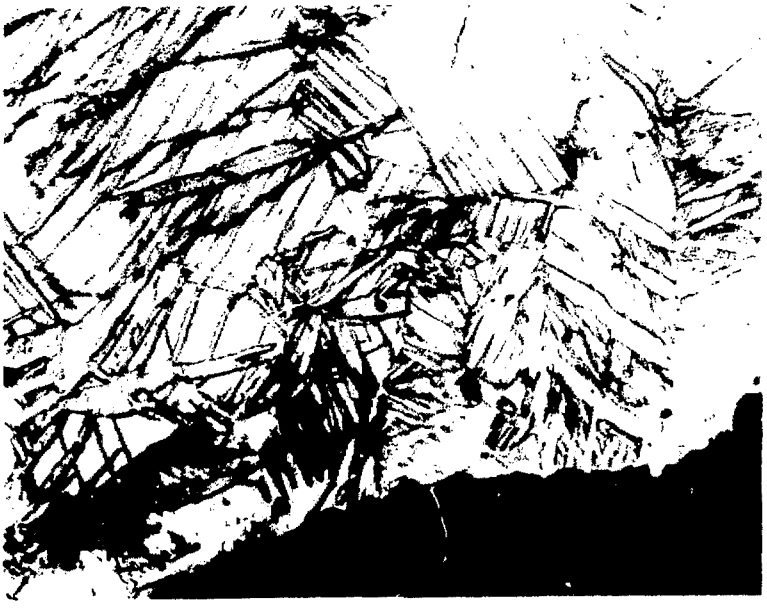

20 μ

Fatigue

Figure 3

XBB 802 2607